IEEE Access
Multidisciplinary ⋮ Rapid Review ⋮ Open Access Journal

Received September 3, 2021, accepted September 20, 2021, date of publication September 23, 2021,
date of current version October 1, 2021.

Digital Object Identifier 10.1109/ACCESS.2021.3115236

A Novel Switched Control Scheme for the Mixed Road in the Lattice Hydrodynamic Model

JIN WAN AND MIN ZHAO
School of Science, Nantong University, Jiangsu 226019, China
Corresponding author: Min Zhao (zhao.m@ntu.edu.cn)

This work was supported in part by the National Natural Science Foundation of China under Grant 61903203.

ABSTRACT Based on the common existence of the mixed road, a switched controller with consideration of the difference between estimation optimal and current flux (EOCFD) is presented in the lattice hydrodynamic model of traffic flow. Based on the Hurwitz criteria and the H_∞-norm, stability conditions for the curved road and straight road scenarios are obtained with the transfer functions G_0 and G_1 respectively. By analyzing the Bode-plot of transfer functions G_0 and G_1, stability analysis is performed with the feedback gain k, the radian θ_j and the curvature radius R. These theoretical results indicate that the switched control scheme prompts the traffic flow to be more stable in both curved and straight roads. Compared with Cheng's model, numerical simulations with multiple perturbations confirm that the switched control scheme can further suppress the traffic congestion with a lower feedback gain on mixed road.

INDEX TERMS Switched control, mixed road, lattice hydrodynamic model, traffic flow.

I. INTRODUCTION

With the rapid urbanization development and car ownership growth, the traffic jam problem has attracted tremendous attention and becomes a topic issue in the last few decades. To increase the efficiency of limited transport resources, various traffic models have been presented to reveal the mechanism of traffic jams. These traffic models generally fall into two categories: macroscopic [1]–[4] and microscopic [5]–[9] traffic flow models. The microscopic models mainly focus on the dynamic behaviour of individual vehicles. While the macroscopic models ignore individual characteristics and describe traffic flow characteristics with density, flow and velocity variables.

By incorporating the ideas of macroscopic as well as microscopic traffic flow models, a lattice hydrodynamic model [10] was firstly established to analyze density waves of traffic jams on straight road. And the modified Korteweg-de Vries (mKdV) equation was also derived to describe the nonlinear evolution of traffic jams near the critical point. Considering the actual traffic complexity, many extended lattice hydrodynamic models have been developed under various scenarios, such as the two-lane road [11], [12], the gradient road [13], [14] and the curved road [15]–[18], etc. When turning corners, the trajectory of the vehicle is susceptible to the radian, the friction coefficient, the curvature radius and so on. This means more influence factors should be further addressed in the stability analysis of curved road ones, which are quite different from straight road cases. In 2016, Zhou and Shi [15] put forward a lattice hydrodynamic model on curved road through the linear and nonlinear stability analysis. Based on this single-lane case, Zhou *et al.* [16] further investigated a two-lane lattice hydrodynamic model on curved road and revealed the lane-changing effect on the stability of traffic flow. Wang *et.al.* [18] also analyzed the traffic flow stability on curved road from the perspective of the driver's memory effect and difference of optimal velocity.

With the rapid development of wireless communication technology and control theory, many traffic control strategies have been applied in lattice hydrodynamic models. For example, under the straight road framework, feedback controllers have been conducted with various traffic information such as the flux difference [19], the historic density difference [20], the next-nearest-neighbor interactions [21], the difference between estimation optimal and current flux (EOCFD) [22], [23] and so on. However, the studies for lattice hydrodynamic models with traffic control strategies under the curved road framework are still infrequent. Although Cheng and Wang [24] proposed a new lattice model on a mixture of straight and curved roads, the control scheme shared the same form on mixed road.

The associate editor coordinating the review of this manuscript and approving it for publication was Jie Gao.

Switching control strategy [25]–[31] has been typically applied in hybrid systems which are composed of several subsystems and a switching law among them. An important feature of switching control is that different controllers can be selected according to the switching law to obtain better control performance. The architecture for such a multi-controller switched system is shown in Fig. 1. In fact, it is much expected that vehicles can automatically adopt the corresponding control scheme according to the type of the mixed road. The aim of this paper is to provide a novel insight on how to utilize the switching control conception to effectively analyze the characteristics of traffic flow on mixed road.

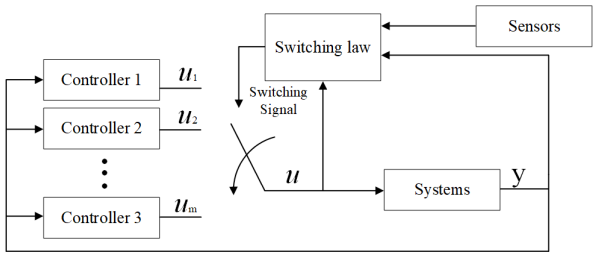

FIGURE 1. Switching control flow chart.

II. THE EXTENDED MODEL WITH A CONTROL SCHEME

In 1998, Nagatani [10] proposed the first lattice hydrodynamic model to describe the evolution of traffic flow on straight road. And the continuity equation and evolution equation are given as follows:

$$\partial_t \rho_j + \rho_0 \left(\rho_j v_j - \rho_{j-1} v_{j-1}\right) = 0 \tag{1}$$

$$\partial_t q_j = a\left[\rho_0 V_s\left(\rho_{j+1}\right) - \rho_j v_j\right], \tag{2}$$

where ρ_j denotes the local density on straight road. ρ_0 and a represent the average density and the sensitivity of drivers, respectively. The optimal velocity function $V_s(\cdot)$ is adopted as

$$V_s(\rho) = \frac{v_{\max}}{2}\left[\tanh\left(\frac{1}{\rho} - \frac{1}{\rho_c}\right) + \tanh\left(\frac{1}{\rho_c}\right)\right], \tag{3}$$

where $v_{max} = 2\ m/s$ denotes the maximal velocity and $\rho_c = 0.25\ m^{-1}$ indicates the critical density. $V_s(\cdot)$ is monotonically decreasing with a turning point at $\rho = \rho_c$.

Fig. 2 is the movement of vehicles running on curved road. The curved road is obtained as $y = \sqrt{R^2 - (x-R)^2}$, where R represents the curvature radius. The distance l between lattice j and $j-1$ is

$$l = \int_{x-x_0}^{x} \sqrt{1 + y'^2}\, dx \approx \frac{x_0}{\sin\theta_j}, \tag{4}$$

where θ_j indicates the radian at lattice j and x_0 means the average headway on straight road.

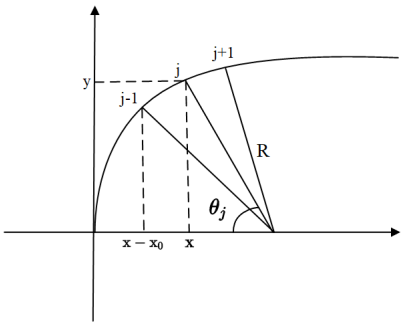

FIGURE 2. The movement of vehicles running on curved road.

The conservation equation is rewritten by incorporating the curved road factor as follows [15]:

$$\partial_t r_j + \frac{\rho_0}{\sin\theta_j}\left(\rho_j v_j - \rho_{j-1} v_{j-1}\right) = 0, \tag{5}$$

where r_j and $\frac{\rho_0}{sin\theta_j}$ denote the local density and the average density on curved road, respectively. And the corresponding optimal velocity function can be expressed as

$$V_r(r_j) = m\frac{\sqrt{\mu g R}}{2}\left\{\tanh\left[\frac{2}{r_0} - \frac{r_j}{r_0^2} - \frac{1}{r_c}\right] + \tanh\left(\frac{1}{r_c}\right)\right\}, \tag{6}$$

where r_c and r_0 denote the critical density and the average density, respectively. $\sqrt{\mu g R}$ is the maximal velocity on curved road. m and μ represent a control parameter of the maximal velocity and a friction coefficient of the curved road, respectively. g is the gravitational acceleration.

From the perspective of control schemes, an extended lattice hydrodynamic model was presented by considering the mixed road [24] as follows:

$$\begin{cases} \partial_t \rho_{j+1} + \rho_0\left(q_{j+1} - q_j\right) = 0 \\ \partial_t r_{j+1} + \lambda\rho_0\left(q_{j+1} - q_j\right) = 0 \\ \partial_t\left(\rho_j v_j\right) = a\left[m\rho_0 V_s\left(\rho_{j+1}\right) + n\rho_0 V_r\left(r_{j+1}\right) - q_j\right] + u_j \\ u_j = k(q_{j+1} - q_j). \end{cases} \tag{7}$$

where $q_j = \rho_j v_j$ is the flux flow. m and n is the ratio of the straight road and curved road. λ is a reaction coefficient and u_j represents a fixed control signal.

In light of the aforementioned facts, Cheng et.al [24] analyzed how the fixed controller u_j stabilized the traffic flow on mixed road. Although the characteristics of the mixed road are reflected in the evolution equation of Eq. (7), the corresponding controllers have not been adopted for different types of roads. The improvement of the vehicle automation capacity has been made possible by the rapid development of communication technology and sensor technology. Given the diversity of the mixed road, what deserves to expect is that vehicles can automatically select the corresponding controller with the assistance of sensor technology. In the case of the mixed road, a novel lattice model with the consideration of a

switched EOCFD controller is firstly proposed as follows:

$$\begin{cases} \partial_t \rho_j + \rho_0 \left(q_{j+1} - q_j\right) = 0 \\ \partial_t r_j + \dfrac{\rho_0}{\sin\theta_j}\left(q_{j+1} - q_j\right) = 0 \\ \partial_t \left(q_j\right) = a\left[\beta\rho_0 V_s(\rho_{j+1}) + (1-\beta)\dfrac{\rho_0}{\sin\theta_j} V_r\left(r_{j+1}\right) - q_j\right] \\ +u_{j,\beta} \\ u_{j,\beta} = k\beta\left(\rho_0 V_s\left(\rho_0\right) - q_j\right) \\ +k\left(1-\beta\right)\left(\dfrac{\rho_0}{sin\theta_j} V_r\left(\dfrac{\rho_0}{sin\theta_j}\right) - q_j\right), \end{cases} \tag{8}$$

where $u_{j,\beta}$ represents a switched controller. $\rho_0 V_s\left(\rho_0\right) - q_j$ means the difference between estimation optimal and current flux on straight road. Likewise, $\frac{\rho_0}{sin\theta_j} V_r\left(\frac{\rho_0}{sin\theta_j}\right) - q_j$ is the EOCFD effect term on curved road. k and β denote the feedback gain and a switched index, respectively. The following switching laws are selected as follows:

When $\beta = 1$, it indicates that the feature of the straight road is identified by sensor technology. Then, the control signal $u_{j,\beta}$ switches to the EOCFD controller of the straight case; When $\beta = 0$, it indicates that the feature of the curved road is identified and the control signal $u_{j,\beta}$ switches to the EOCFD controller of the curved case.

The optimal velocity function OV on straight road is chosen as the same as Eq.(3). And Eq. (6) is also selected as the adopted optimal velocity function OV on curved road in this paper.

III. CONTROL THEORY ANALYSIS

In this section, the control theory is adopted to discuss how the switched controller suppresses traffic jams on mixed road.

Assume that ρ^* and r^* are the desired density of the straight road and that of the curved road, respectively. And the desired flux of the traffic flow is q^*. Thus, the steady-state uniform flow solutions for the traffic system are defined as

$$[\rho_n, q_n]^T = \left[\rho^*, q^*\right]^T, \tag{9}$$

$$[r_n, q_n]^T = \left[r^*, q^*\right]^T. \tag{10}$$

The controlled traffic system of Eq.(8) can be linearized under small perturbations $\left[\rho^0, q^0\right]$ and $\left[r^0, q^0\right]$ as follows:

$$\begin{cases} \partial_t \rho^0_{j+1} + \rho_0\left(q^0_{j+1} - q^0_j\right) = 0 \\ \partial_t r^0_{j+1} + \dfrac{\rho_0}{\sin\theta_j}\left(q^0_{j+1} - q^0_j\right) = 0 \\ \partial_t q^0_j = a\left[\beta\rho_0\Lambda_1\rho^0_{j+1} + (1-\beta)\dfrac{\rho_0}{\sin\theta_j}\Lambda_2 r^0_{j+1} - q^0_j\right] \\ \qquad + u^0_{j,\beta} \\ u^0_{j,\beta} = k\beta(-q^0_j) + k(1-\beta)(-q^0_j) = -kq^0_j. \end{cases} \tag{11}$$

Simplifying Eq.(11), the novel controller can be deduced as

$$\partial_t q^0_j = a\left\{\beta\rho_0\Lambda_1\rho^0_{j+1} + (1-\beta)\frac{\rho_0}{\sin\theta_j}\Lambda_2 r^0_{j+1} - q^0_j\right\} - kq^0_j, \tag{12}$$

where $\rho^0_{j+1} = \rho_{j+1} - \rho^*$, $q^0_j = q_j - q^*$, $q^0_{j+1} = q_{j+1} - q^*$, $\Lambda_1 = \left.\frac{\partial V_s(\rho_{j+1})}{\partial\rho_{j+1}}\right|_{\rho_{j+1}=\rho^*}$, $\Lambda_2 = \left.\frac{\partial V_r(r_{j+1})}{\partial r_{j+1}}\right|_{r_{j+1}=r^*}$.

By performing Laplace transformation and Taylor expansion on Eq.(11), one can obtain

$$\begin{cases} sP_{j+1}(s) - \rho_{j+1}(0) + \rho_0\left[Q_{j+1}(s) - Q_j(s)\right] = 0 \\ sR_{j+1}(s) - r_{j+1}(0) + \dfrac{\rho_0}{\sin\theta_j}\left[Q_{j+1}(s) - Q_j(s)\right] = 0 \\ sQ_j(s) - q_j(0) = a\{\beta\rho_0\Lambda_1 P_{j+1}(s) \\ +(1-\beta)\dfrac{\rho_0}{\sin\theta_j}\Lambda_2 R_{j+1}(s) - Q_j(s)\} - kQ_j(s), \end{cases} \tag{13}$$

where $P_{j+1}(s) = \mathcal{L}(\rho_{j+1})$, $Q_j(s) = \mathcal{L}(q_j)$, $Q_{j+1}(s) = \mathcal{L}(q_{j+1})$, $R_{j+1}(s) = \mathcal{L}(r_{j+1})$. $\mathcal{L}(\cdot)$ and s indicate the Laplace transform and a complex variable, respectively.

By eliminating the variable $P_{j+1}(s)$ of Eq.(13), the flux equation between $Q_j(s)$ and $Q_{j+1}(s)$ can be expressed as

$$Q_j(s) = \frac{-a\beta\rho_0^2\Lambda_1 - a(1-\beta)\frac{\rho_0^2}{\sin^2\theta_j}\Lambda_2}{s^2 + s(k+a) - a\beta\rho_0^2\Lambda_1 - a(1-\beta)\frac{\rho_0^2}{\sin^2\theta_j}\Lambda_2} Q_{j+1}(s), \tag{14}$$

where $D(s)$ signifies the characteristic polynomial. The polynomial is equal to $s^2 + s(k+a) - a\beta\rho_0^2\Lambda_1 - a(1-\beta)\frac{\rho_0^2}{\sin^2\theta_j}\Lambda_2$. Based on the Hurwitz stability criterion, it is known that $D(s)$ remains stable when $\Lambda_1 < 0$, $\Lambda_2 < 0$ and $k + a > 0$.

Thus, the transfer function $G(s)$ can be described as

$$G(s) = \frac{-a\beta\rho_0^2\Lambda_1 - a(1-\beta)\frac{\rho_0^2}{\sin^2\theta_j}\Lambda_2}{D(s)}. \tag{15}$$

Based on the control theory [32], traffic congestions never occur in the traffic flow if and only if the following conditions can be satisfied:

(1) The characteristic polynomial $D(s)$ is stable;

(2) The H_∞ norm of transfer function $||G(s)||_\infty \leq 1$ for any $\omega > 0$.

In summary, the stability criterion of Eq.(8) can be obtained as follows:

$$\begin{cases} \|G(s)\|_\infty = \sup_{w\in[0,\infty)} |G(jw)| \leq 1 \\ |G(jw)| = \sqrt{G(jw)G(-jw)} = \\ \sqrt{\dfrac{\left(a\beta\rho_0^2\Lambda_1 + a(1-\beta)\frac{\rho_0^2}{sin\theta_j^2}\Lambda_2\right)^2}{\left(a\beta\rho_0^2\Lambda_1 + a(1-\beta)\frac{\rho_0^2}{sin\theta_j^2}\Lambda_2 + \omega^2\right)^2 + (a+k)^2\omega^2}} \leq 1. \end{cases} \tag{16}$$

Case 1: If $\beta = 1$, the transfer function $G_1(s)$ of the straight road can be given by

$$|G_1(j\omega)| = \sqrt{G_1(j\omega)G_1(-j\omega)} = \sqrt{\frac{\left(a\rho_0^2\Lambda_1\right)^2}{\left(a\rho_0^2\Lambda_1 + \omega^2\right)^2 + (a+k)^2 w^2}} \leqslant 1, \tag{17}$$

where $g_1(\omega) = \frac{(a\rho_0^2\Lambda_1)^2}{(a\rho_0^2\Lambda_1+\omega^2)^2+(a+k)^2w^2}$. Obviously, $g_1(0) = 1$ and $g_1(\omega) \leq 1$. The following inequality equation could be obtained as follows:

$$\omega^2 + 2a\rho_0^2\Lambda_1 + (a+k)^2 \geq 0. \tag{18}$$

Consequently, the stability condition corresponding to Eq.(18) is

$$a \geq \sqrt{2k\Lambda_1\rho_0^2 + \Lambda_1^2\rho_0^4} - k - \Lambda_1\rho_0^2. \tag{19}$$

Case 2: If $\beta = 0$, the transfer function $G_0(s)$ of the curved road can be given by

$$|G_0(j\omega)| = \sqrt{G_0(j\omega)G_0(-j\omega)} = \sqrt{\frac{\left(a\frac{\rho_0^2}{\sin^2\theta_j}\Lambda_2\right)^2}{\left(a\frac{\rho_0^2}{\sin^2\theta_j}\Lambda_2 + \omega^2\right)^2 + (a+k)^2 w^2}} \leqslant 1, \tag{20}$$

where $g_0(\omega) = \frac{\left(a\frac{\rho_0^2}{\sin^2\theta_j}\Lambda_2\right)^2}{\left(a\frac{\rho_0^2}{\sin^2\theta_j}\Lambda_2+\omega^2\right)^2+(a+k)^2w^2}$. Obviously, $g_0(0) = 1$ and $g_0(\omega) \leq 1$. The following inequality equation could be obtained as follows:

$$\omega^2 + 2a\frac{\rho_0^2}{sin^2\theta_j}\Lambda_2 + (a+k)^2 \geq 0. \tag{21}$$

Consequently, the stability condition corresponding to Eq.(21) is

$$a \geq \frac{1}{2}\left(\sqrt{\left(\frac{2\Lambda_2\rho_0^2}{\sin^2\theta_j} + 2k\right)^2 - 4k^2} - \frac{2\Lambda_2\rho_0^2}{\sin^2\theta_j} - 2k\right). \tag{22}$$

In addition, when $\theta_j = \pi/2$, the stability condition (19) for the curved road will be equivalent to the one (22) for the straight road.

Fig. 3 depicts the solid Bode curves with different parameters including the feedback gain k, the radian θ_j and the curvature radius R on mixed road. The model stability depends upon the peak value of the Bode curve. The more the peak value deviates from 1, the more the traffic system deviates from the stable state [21].

The Bode-plot Fig. 3(a)-(b) can be obtained by using Eq. (17) and Eq. (20) respectively. Fig. 3(a) demonstrates the amplitude variation of the transfer function $|G_1(s)|$ with different values of k under the straight road scenario. While Fig. 3(b) shows the amplitude of the transfer function $|G_0(s)|$ with the fixed curvature radius $R = 10$ and the radian $\theta_j = \pi/3$ under the curved road scenario. Since the parameters of six solid curves ($k = 0, 0.15, 0.3$) in Fig. 3(a)-(b) do not

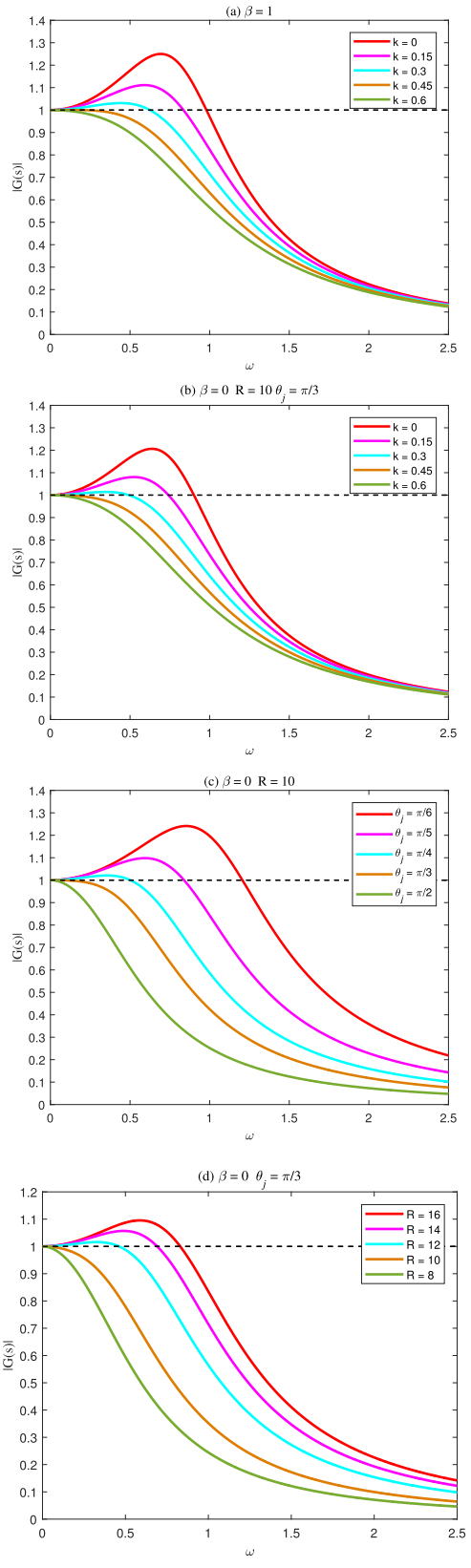

FIGURE 3. Bode-plot for different values of the feedback gain k, the radian θ_j and the curvature radius R.

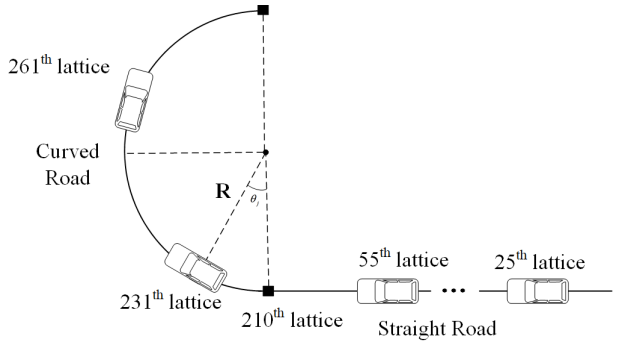

FIGURE 4. The movement of vehicles on mixed road.

satisfy the stability conditions (18) and (21), the peak values of six Bode curves are greater than 1, which will lead to the congested traffic flow. From Fig. 3(a)-(b), it can also be found that the amplitude of the transfer function $|G_1(s)|$ or $|G_0(s)|$ decays gradually with the increased feedback gain k. When $k = 0.45, 0.6$, the stability conditions (17) and (20) corresponding to the straight road and the curved road cases are all satisfied. Then, the instability of traffic flow will die out and the traffic flow evolves into the uniform flow.

In view of the curved road scenario, Fig. 3(c) shows the amplitude of transfer function $|G_0(s)|$ with different values of the radian θ_j. When the fixed parameter $R = 10$ and the radian θ_j equals to $\pi/6, \pi/5, \pi/4$, the peak values of the Bode curves are about 1.25, 1.1, 1.03, respectively. However, when the radian θ_j equals to $\pi/3, \pi/2$, all values of the Bode curves are smaller than 1. This indicates that the traffic flow stability enhances with the continuous growing value of θ_j. As soon as $\theta_j = \pi/3$, the peak value of the transfer function $|G_0(s)|$ is smaller than 1, which means that the traffic flow reaches its desired steady flux.

Fig. 3(d) displays the variation trend of the Bode curves for different values of the curvature radius R with a fixed parameter $\theta_j = \pi/3$. It is obvious that the amplitude of $|G_0(s)|$ is weaker with the decreasing value of R. This reveals that there is a negative correlation between the curvature radius R and the stability of traffic flow. From Fig. 3 (c)-(d), it can also be found that the effect parameters θ_j and R have on the traffic flow stability coincides with the ones in [15], [16].

Generally speaking, the increase of the radian θ_j is conducive to the stability of traffic flow. While the increased curvature radius R is detrimental to the uniform stability of traffic flow.

IV. NUMERICAL SIMULATION

In this section, a switched EOCFD controller is applied in the lattice hydrodynamic model on mixed road. Following the [24], the ratio of the straight road and the curved road are set as $m = 0.7$ and $n = 0.3$. Assume the mixed road in Fig. 4 is divided into 300 lattices. Then, the lattices from 1^{th} to 210^{th} represent the straight part, while the lattices from 211^{th} to 300^{th} represent the curved one. The related parameters in the fixed controller and the switched EOCFD controller are

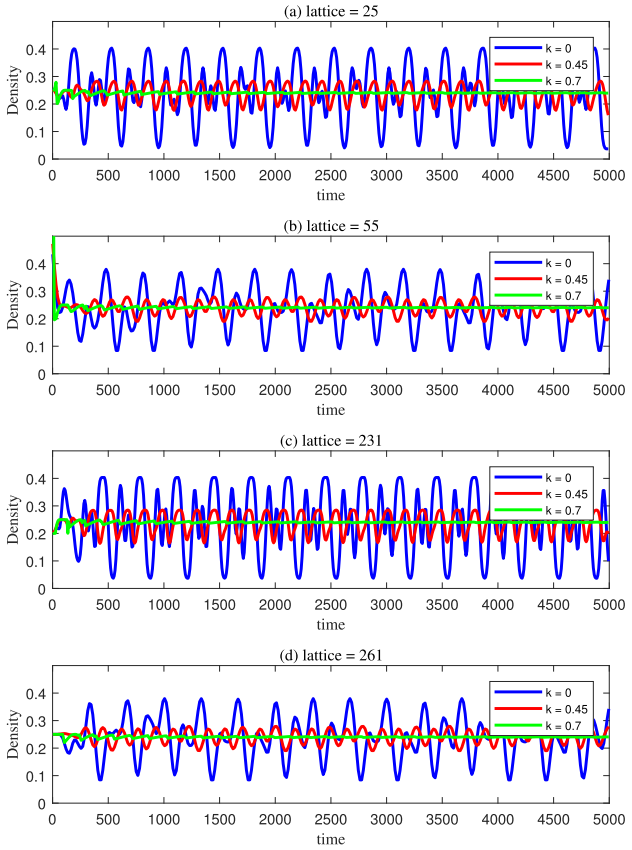

FIGURE 5. Density-time plot for lattices $j = 25, 55, 231, 261$ with different values of the feedback gain k and $R = 10$ in Cheng's model.

chosen as $\rho_c = \rho_0 = 0.25$, $a = 1.5$, $t = 5000s$, $v_{max} = 2$, $m = 1.4$, $\mu = 0.9$ and $r_c = 0.1$. The initial conditions of the density ρ_j on straight road and the density r_j on curved road are selected as follows:

$$\begin{aligned} \rho_j(0) &= \rho_0 = 0.25(1 \le j \le 210) \\ r_j(0) &= r_0 = 0.2(211 \le j \le 300) \end{aligned} \tag{23}$$

And the initial multiple perturbations on mixed road are given by

$$\begin{aligned} \rho_j(1) &= \begin{cases} 0.5 & 50 \le j \le 55 \\ 0.2 & 55 < j \le 60 \\ 0.25 & j < 50, 60 < j \le 210 \end{cases} \\ r_j(1) &= 0.2, 211 \le j \le 300 \end{aligned} \tag{24}$$

For the sake of simplicity, representative values of R, k, θ_j and lattice sites have been adopted to further validate the effectiveness of theoretical analysis in Section III.

To further validate the effectiveness of the switched EOCFD controller on mixed road, simulations are carried out with periodic boundary conditions for two cases:

Case 1: The fixed controller on mixed road

Fig. 5 exhibits the density waves under the fixed controller (7) on mixed road with the curvature radius $R = 10$ for $t = 1 - 5000s$. Moreover, Fig. 5(a)-(b) show the density-time plot with different feedback gains k at two representative

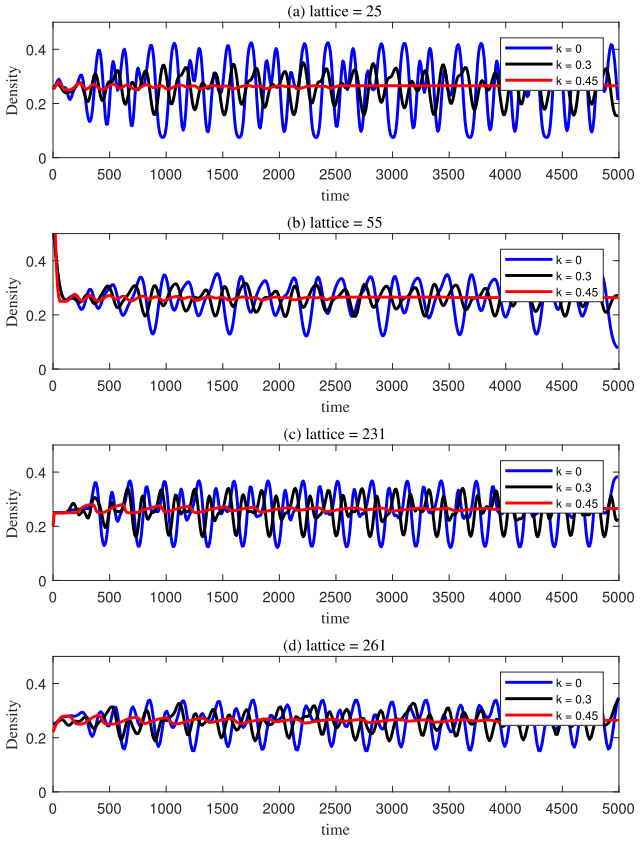

FIGURE 6. Density-time plot for lattices $j = 25, 55, 231, 261$ with different values of the feedback gain k, $R = 10$ and $\theta_j = \pi/3$ in the novel model.

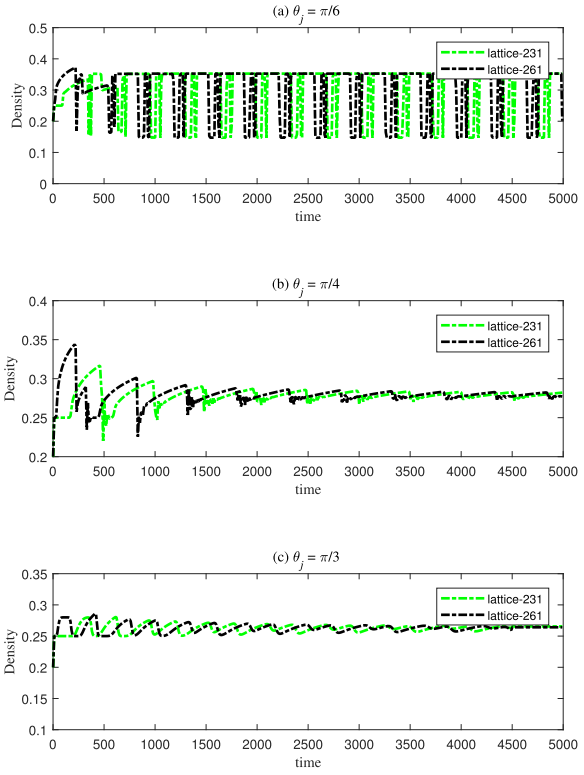

FIGURE 7. Density-time plot for different values of the radian θ_j with $\beta = 0$, $k = 0.45$ and $R = 10$ on curved road.

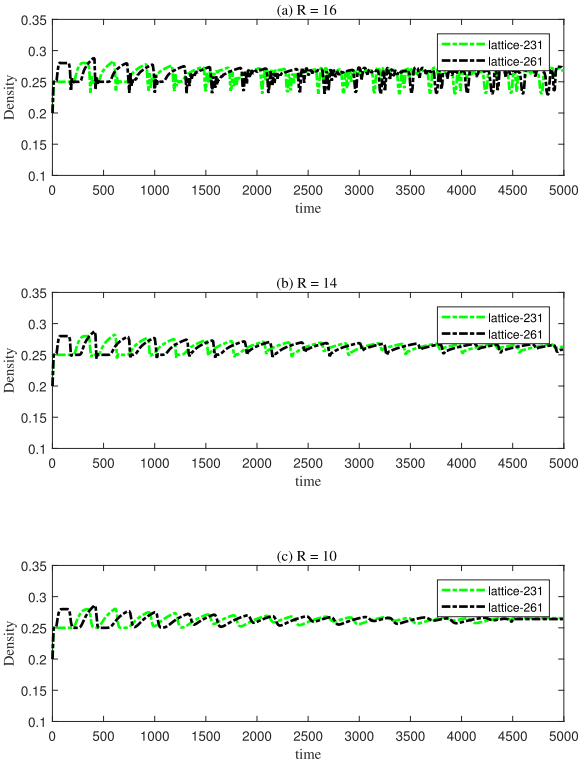

FIGURE 8. Density-time plot for different values of the curvature radius R with $\beta = 0$, $k = 0.45$ and $\theta = \pi/3$ on curved road.

lattices on straight road. While Fig. 5(c)-(d) demonstrate the density-time plot at the other two representative lattices on curved road. Obviously, the oscillation amplitude of density waves for any position of lattice in Fig. 5 all deteriorates gradually with the increasing value of the feedback gain k. Additionally, whether on straight road or curved road, the oscillation amplitude of the density wave falls into the steady state with $k = 0.7$.

Case 2: The switched controller on mixed road

Different from the fixed controller (7), the switched control scheme (8) can be automatically switched according to the type of the mixed road. Fig. 6 (a)-(b) and Fig. 6 (c)-(d) reveal the density-time plot of lattices on straight road and curved road, respectively. Similar to Fig. 5, the feedback gain k also has positive influence on traffic stability of the mixed road. When $\theta_j = \pi/3$ and $R = 10$, the oscillation of density waves at different lattices in Fig. 6 all becomes slighter with the increasing value of k. Particularly when $k = 0.45$, the fluctuations of density waves for four different lattices in Fig. 6 die out and the traffic flow falls into the steady-state finally.

Note that the density waves of red curves ($k = 0.45$) in Fig. 5 remain in an unstable state. Compared with the fixed controller (7), the novel switched control scheme (8) can be more favorable to the stability enhancement of the traffic system on mixed road with a lower feedback control gain.

Additionally, Figs. 7-8 further demonstrate how the radian θ_j and the curvature radius R affect the traffic flow stability only on curved road.

Fig. 7 demonstrates the profile density for different values of the radian θ_j with the fixed $R = 10$ and $k = 0.45$. As the stability condition (22) of the curved road is not satisfied, these small perturbations evolve into the congested flow in Fig. 7(a)-(b). When $\theta_j = \pi/3$, the stability condition of traffic flow is satisfied after time $t = 4500s$. This leads to the traffic state changing from an unstable state to a stable state, as shown in Fig.7(c). In other words, the increased radian θ_j contributes to the improvement of the traffic flow stability.

Fig. 8 depicts the evolution of traffic density with different values of the curvature radius R when $\theta_j = \pi/3$ and $k = 0.45$. When the curvature radius R is set as 16, the range of amplitude fluctuation is about 0.2 to 0.3 in Fig. 8(a).

And the fluctuation of density waves tends to be gentle gradually in Fig. 8(b). When R decreases to 10, the oscillation of the density wave is reduced and reaches the steady-state after time $t = 4500s$. This reveals that the curvature radius R has negative influence on the traffic flow stability.

In summary, the traffic flow will become stable with the increased radian θ_j or with the decreased curvature radius R. These characteristics of density waves on curved road shown in Fig. 7 and Fig. 8 further validate the theoretical analysis results demonstrated in Fig. 3(c) and Fig. 3(d). On the whole, the proposed feedback control model with consideration of a switched scheme is conducive to relieve the traffic congestion not only on straight road but also on curved road.

V. CONCLUSION

Accounting for the mixed road consisting of curved and straight roads, a new switched controller with consideration of the EOCFD effect is proposed in this study. Through control theory analysis, stability conditions are respectively obtained by the transfer function G_0 and the transfer function G_1. The Bode-plot of transfer functions G_0 and G_1 illustrates that the feedback gain, the curvature radius and the radian play a significant role in the stability of the traffic flow. To verify the effectiveness of the switched EOCFD controller on mixed road, the numerical simulation of the fixed controller has been performed. Compared with the fixed control scheme, it can be concluded that the novel switched control scheme can be more favorable to the stability enhancement of the traffic system with a lower feedback control gain. Moreover, enlarging the radian or reducing the curvature radius may contribute to the stability of traffic flow on curved road. Future work will focus on the improvement of the novel switched control scheme from various respects, such as the decentralized delayed-feedback control, the adaptive fuzzy control signal, and the asynchronous switching.

REFERENCES

[1] G. Zhang and G.-H. Peng, "Research on the stabilization effect of continuous self-delayed traffic flux in macro traffic modeling," *Phys. A, Stat. Mech. Appl.*, vol. 526, Jul. 2019, Art. no. 121012.

[2] R. Cheng, H. Ge, and J. Wang, "An extended macro traffic flow model accounting for multiple optimal velocity functions with different probabilities," *Phys. Lett. A*, vol. 381, no. 32, pp. 2608–2620, 2017.

[3] Y. Liu and C. K. Wong, "A two-dimensional lattice hydrodynamic model considering shared lane marking," *Phys. Lett. A*, vol. 384, no. 27, Sep. 2020, Art. no. 126668.

[4] Y. Chang and R. Cheng, "Effect of speed deviation and anticipation effect of flux difference in the lattice hydrodynamic model," *Phys. A, Stat. Mech. Appl.*, vol. 531, Oct. 2019, Art. no. 121751.

[5] T. Tang, H. Huang, S. C. Wong, and R. Jiang, "A car-following model with the anticipation effect of potential lane changing," *Acta Mechanica Sinica*, vol. 24, no. 4, pp. 399–407, Aug. 2008.

[6] M. Ma, G. Ma, and S. Liang, "Density waves in car-following model for autonomous vehicles with backward looking effect," *Appl. Math. Model.*, vol. 94, pp. 1–12, Jun. 2021.

[7] W.-X. Zhu and L.-D. Zhang, "Analysis of car-following model with cascade compensation strategy," *Phys. A, Stat. Mech. Appl.*, vol. 449, pp. 265–274, May 2016.

[8] Z. Wen-Xing and Z. Li-Dong, "A new car-following model for autonomous vehicles flow with mean expected velocity field," *Phys. A, Stat. Mech. Appl.*, vol. 492, pp. 2154–2165, Feb. 2018.

[9] H. Kuang, Z.-P. Xu, X.-L. Li, and S.-M. Lo, "An extended car-following model accounting for the average headway effect in intelligent transportation system," *Phys. A, Stat. Mech. Appl.*, vol. 471, pp. 778–787, Apr. 2017.

[10] T. Nagatani, "Modified KdV equation for jamming transition in the continuum models of traffic," *Phys. A, Stat. Mech. Appl.*, vol. 261, pp. 599–607, Dec. 1998.

[11] C. Zhu, S. Zhong, and S. Ma, "Two-lane lattice hydrodynamic model considering the empirical lane-changing rate," *Commun. Nonlinear Sci. Numer. Simul.*, vol. 73, pp. 229–243, Jul. 2019.

[12] S. Sharma, "Effect of driver's anticipation in a new two-lane lattice model with the consideration of optimal current difference," *Nonlinear Dyn.*, vol. 81, no. 1, pp. 991–1003, Jul. 2015.

[13] J.-L. Cao and Z.-K. Shi, "Analysis of a novel two-lane lattice model on a gradient road with the consideration of relative current," *Commun. Nonlinear Sci. Numer. Simul.*, vol. 33, pp. 1–18, Apr. 2016.

[14] Q. Wang, R. Cheng, and H. Ge, "A new lattice hydrodynamic model accounting for the traffic interruption probability on a gradient highway," *Phys. Lett. A*, vol. 383, no. 16, pp. 1879–1887, 2019.

[15] J. Zhou and Z.-K. Shi, "Lattice hydrodynamic model for traffic flow on curved road," *Nonlinear Dyn.*, vol. 83, no. 3, pp. 1217–1236, Feb. 2016.

[16] J. Zhou, Z.-K. Shi, and C.-P. Wang, "Lattice hydrodynamic model for two-lane traffic flow on curved road," *Nonlinear Dyn.*, vol. 85, no. 3, pp. 1423–1443, 2016.

[17] Y.-D. Jin, J. Zhou, Z.-K. Shi, H.-L. Zhang, and C.-P. Wang, "Lattice hydrodynamic model for traffic flow on curved road with passing," *Nonlinear Dyn.*, vol. 89, no. 1, pp. 107–124, Mar. 2017.

[18] Q. Wang, R. Cheng, and H. Ge, "A novel lattice hydrodynamic model accounting for driver's memory effect and the difference of optimal velocity on curved road," *Phys. A, Stat. Mech. Appl.*, vol. 559, Dec. 2020, Art. no. 125023.

[19] S. Qin, Z. He, and R. Cheng, "An extended lattice hydrodynamic model based on control theory considering the memory effect of flux difference," *Phys. A, Stat. Mech. Appl.*, vol. 509, pp. 809–816, Nov. 2018.

[20] G. Peng, S. Yang, and L. Qing, "Feedback control pattern for a new lattice hydrodynamic model accounting for historic evolution information," *Int. J. Control*, vol. 93, no. 10, pp. 2370–2377, Dec. 2018.

[21] B.-L. Cen, Y. Xue, Y.-C. Zhang, X. Wang, and H.-D. He, "A feedback control method with consideration of the next-nearest-neighbor interactions in a lattice hydrodynamic model," *Phys. A, Stat. Mech. Appl.*, vol. 559, Dec. 2020, Art. no. 125055.

[22] G. Peng, S. Yang, D. Xia, and X. Li, "A novel lattice hydrodynamic model considering the optimal estimation of flux difference effect on two-lane highway," *Phys. A, Stat. Mech. Appl.*, vol. 506, pp. 929–937, Sep. 2018.

[23] Z. Yicai, Z. Min, S. Dihua, Z. Zhaomin, and C. Dong, "A new feedback control scheme for the lattice hydrodynamic model with drivers' sensory memory," *Int. J. Modern Phys. C*, vol. 32, pp. 1–12, Feb. 2020.

[24] R. Cheng and Y. Wang, "An extended lattice hydrodynamic model considering the delayed feedback control on a curved road," *Phys. A, Stat. Mech. Appl.*, vol. 513, pp. 510–517, Jan. 2019.

[25] Y. Song, J. Yang, T. Yang, and M. Fei, "Almost sure stability of switching Markov jump linear systems," *IEEE Trans. Autom. Control*, vol. 61, no. 9, pp. 2638–2643, Sep. 2016.

[26] Y. Song, J.-X. Xie, Y.-Q. Shi, and L. Jia, "Switching stabilization for the inverted pendulum system," in *Proc. Chin. Control Decis. Conf.*, Jun. 2009, pp. 1033–1037.
[27] S. Li, C. K. Ahn, and Z. Xiang, "Command-filter-based adaptive fuzzy finite-time control for switched nonlinear systems using state-dependent switching method," *IEEE Trans. Fuzzy Syst.*, vol. 29, no. 4, pp. 833–845, Apr. 2021.
[28] S. Li, C. K. Ahn, and Z. Xiang, "Sampled-data adaptive output feedback fuzzy stabilization for switched nonlinear systems with asynchronous switching," *IEEE Trans. Fuzzy Syst.*, vol. 27, no. 1, pp. 200–205, Jan. 2019.
[29] D. Liberzon and A. S. Morse, "Basic problems in stability and design of switched systems," *IEEE Control Syst.*, vol. 19, no. 5, pp. 59–70, Oct. 1999.
[30] C. Peng and H. Sun, "Switching-like event-triggered control for networked control systems under malicious denial of service attacks," *IEEE Trans. Autom. Control*, vol. 65, no. 9, pp. 3943–3949, Sep. 2020.
[31] C. Peng, J. Wu, and E. Tian, "Stochastic event-triggered H∞ control for networked systems under denial of service attacks," *IEEE Trans. Syst., Man, Cybern. Syst.*, early access, Jul. 1, 2021, doi: 10.1109/TSMC.2021.3090024.
[32] K. Konishi, H. Kokame, and K. Hirata, "Decentralized delayed-feedback control of an optimal velocity traffic model," *Eur. Phys. J. B Condens. Matter Complex Syst.*, vol. 15, no. 4, pp. 715–722, Jun. 2000.

JIN WAN received the B.S. degree in software engineering from Huaiyin Institute of Technology, China, in 2020. She is currently pursuing the master's degree with the School of Science, Nantong University. Her research interests include traffic flow modeling, nonlinear analysis, and traffic control.

MIN ZHAO received the B.Sc. degree in applied mathematics and the M.Sc. degree in software engineering from Soochow University, Suzhou, China, in 2002 and 2005, respectively, and the Ph.D. degree from the School of Mechatronic Engineering and Automation, Shanghai University, Shanghai, China, in 2021. She is currently an Associate Professor with the School of Science, Nantong University, Jiangsu, China. Her research interests include networked control systems, multi-agent systems, and event-triggered control systems.